

Sphere: complete laboratory performance and prediction for on-sky first light

Jean-François Sauvage^{a,b}, Jean-Luc Beuzit^b, Ronald Roelfsema^c, Markus Feldt^d, Kjetil Dohlen^e,
David Mouillet^b, Pascal Puget^b, Francois Wildi^f, Lyu Abe^g, Andrea Baruffolo^h, Pierre Baudozⁱ,
Andreas Bazzon^k, Anthony Boccalettiⁱ, Tristan Buey^l, Marcel Carbillet^g, Julien Charton^b, Riccardo
Claudi^h, Anne Costille^e, Alain Delboulbé^b, Silvano Desidera^h, Carsten Dominik^l, Mark Downing^j,
Christophe Fabron^e, Philippe Feautrier^b, Enrico Fedrigo^j, Thierry Fusco^a, Enrico Giro^h, Laurence
Gluck^b, Raffaele Gratton^h, Thomas Henning^d, Norbert Hubin^l, Markus Kasper^j, Anne-Marie
Lagrange^b, Maud Langlois^m, David Le Mignant^e, Jean-Louis Lizonⁱ, Fabrice Madec^e, Yves
Magnard^b, Patrice Martinez^e, Dino Mesa^h, Ole Möller-Nilsson^d, Thibaut Moulin^b, Claire Moutou^e,
Alexey Pavlov^d, Denis Perretⁱ, Cyril Petit^a, Johan Pragt^c, Patrick Rabou^b, Sylvain Rochat^b, Bernardo
Salasnich^h, Gérard Roussetⁱ, Hans-Martin Schmid^k, Arnaud Sevinⁱ, Christian Soenke^j, Eric Stadler^b,
Marcos Suarez^j, Massimo Turatto^h, Stéphane Udry^f, Arthur Vigan^e, Farrokh Vakili^g, Gérard Zins^b,
Alice Zurlo^e

^a Office National d'Etudes et de Recherches Aérospatiales, B.P. 72, F-92322 Chatillon, France;

^b IPAG, UMR5274, CNRS/Université J. Fourier, B.P. 53, F-38041 Grenoble Cedex 9, France;

^c NOVA/ASTRON, Oude Hoogeveensedijk 4, NL-7990 PD Dwingeloo, The Netherlands;

^d Max Planck Institut für Astronomie, Königstuhl 17, D-69117 Heidelberg, Germany;

^e LAM, UMR6110, CNRS/Université de Provence, B.P. 8, F-13376 Marseille Cedex 12, France;

^f Observatoire de Genève, 51 chemin des Maillettes, CH-1290 Sauverny, Switzerland;

^g Laboratoire Lagrange, UMR7293, UNS/CNRS/OCA, Observatoire de la Côte d'Azur, BP 4229, F-06304 Nice Cedex 4, France;

^h Osservatorio Astronomico di Padova, INAF, Vicolo dell'Osservatorio 5, I-35122 Padova, Italy;

ⁱ LESIA, UMR8109, CNRS/Observatoire de Paris, 5 place J. Janssen, F-92190 Meudon, France;

^j European Southern Observatory, Karl-Schwarzschild-Strasse 2, D-85748 Garching, Germany;

^k Institute of Astronomy, ETH Zurich, CH-8092 Zurich, Switzerland;

^l Universit t van Amsterdam, Kruislaan 403, NL-1098 SJ Amsterdam, The Netherlands

^m CRAL, UMR 5574, CNRS/Universit  C. Bernard, Observatoire de Lyon, 9, avenue Charles-Andr , F-69561 Saint Genis Laval Cedex, France

ABSTRACT

Direct imaging of exoplanet is one of the most exciting field of planetology today. The light coming from exoplanet orbiting their host star witnesses for the chemical composition of the atmosphere, and the potential biomarkers for life. However, the faint flux to be imaged, very close to the huge flux of the parent star, makes this kind of observation extremely difficult to perform from the ground. The direct imaging instruments (SPHERE [1], GPI [2]) are nowadays reaching lab maturity. Such instrument imply the coordination of XAO for atmospheric turbulence real-time correction, coronagraphy for star light extinction, IR Dual band camera, IFS, and visible polarimetry. The imaging modes include single and double difference (spectral and angular). The SPHERE project is now at the end of AIT phase. This paper presents the very last results obtained in laboratory, with realistic working conditions. These AIT results allows one to predict on-sky performance, that should come within the next weeks after re-installation at Very Large Telescope at Paranal.

Keywords: High contrast imaging, extreme adaptive optics, exoplanet direct imaging

1. INTRODUCTION

The primary goal of Extrasolar Planet science of the next decade is a better understanding of the mechanism of formation and evolution of planetary systems. SPHERE will give a primary contribution in this area. Determination of the frequency of giant planets in wide orbits ($> 5\text{-}10$ AU) will allow testing basic aspects of the planet formation models. High-resolution, high contrast imaging like that provided by SPHERE is expected to be the most efficient technique to discover planets in the outer regions of planetary systems. With its enhanced capabilities (a gain of two orders of magnitude in contrast with respect to existing instruments) and a list of potential targets including several hundred stars, SPHERE will provide a clear view of the frequency of giant planets in wide orbits. Both evolved and young planetary systems will be detected, respectively through their reflected light (mostly by visible differential polarimetry [8]) and through the intrinsic planet emission (using IR differential imaging IRDIS [6] and integral field spectroscopy IFS [7]). Beside frequency it would also be interesting to derive the distributions of planets parameters such as mass, semi-major axis and eccentricities. The main scientific goal of SPHERE will be then the description of the properties of young planets in the expected peak region of gas giant formation and in the outer regions of the systems. Furthermore, a direct imager like SPHERE provides the only way of obtaining spectral characteristics for outer planets. Finally, a few planets shining by reflecting stellar light might be detected by the SPHERE polarimetric channel (ZIMPOL). SPHERE will be then highly complementary to current and contemporaneous studies of extrasolar planets.

The present paper presents the status of the SPHERE instrument in section 2, then demonstrates the system performance in section 3, and ends up with a study of the relevance of a laboratory demonstration for an instrument dedicated to complex sky observations in section 4.

2. SPHERE OVERVIEW

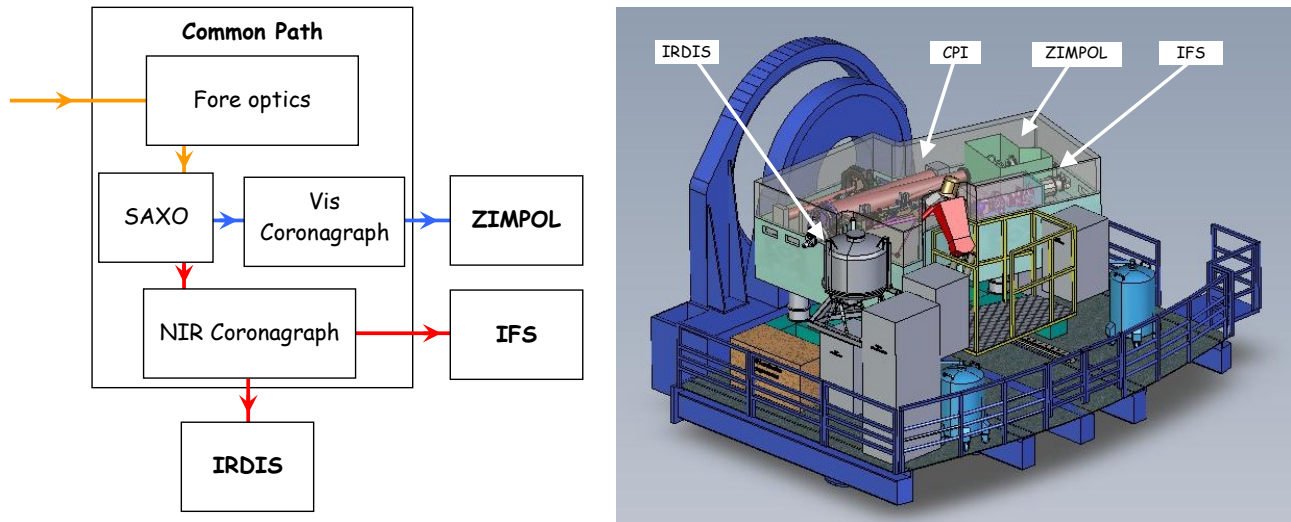


Figure 1 SPHERE four sub-systems

Including in the common path (CPI) the high order adaptive optics system (SAXO), coronagraphs, and the three observing subsystems IRDIS, IFS and ZIMPOL (see text). Left: block diagram. Right: schematic view on the Nasmyth platform.

The SPHERE instrument lies on the VLT Nasmyth platform and is divided into four subsystems (Figure 1):

- The Common Path and Infrastructure (CPI) receives the light from the telescope, supports the 3 other sub-systems and feed them with highly stabilized, AO-corrected and coronagraphic beams.
- ZIMPOL produces either images or differential polarimetric images in the visible range.
- The integral field spectrograph (IFS) produces spectra on each point of the internal FoV in NIR.
- The infrared dual-band imager and spectrograph (IRDIS) also works in NIR with a larger FoV and various modes: classical imaging (CI), dual-band imaging (DBI), dual-polarization imaging (DPI), or long slit spectroscopy (LSS).

The whole SPHERE design and its more severe specifications have been driven by the primary science case of exoplanet imaging (wide and efficient detection surveys and characterization capabilities). It provides a very high image quality of a narrow field around bright targets (corrected from turbulence and highly stabilized) that can be observed in visible or near infrared. Observations can be made without or with a variety of coronagraphs.

In visible with ZIMPOL, imaging (centered on the bright star or offset up to a radius of $4''$) is possible in a variety of narrow band to broad band filters, down to 15 mas diffraction-limited angular resolution obtained in good conditions of AO turbulence correction. Interestingly, very accurate differential polarimetric imaging, obtained quasi-simultaneously by fast modulation, can reveal very faint circumstellar linearly polarized light (such as reflected light). ZIMPOL cannot be used simultaneously with the other sub-systems IFS or IRDIS in the NIR.

This imager IRDIS can also be used alone in the following modes:

- Dual-band imaging (DBI) with other pairs of filters, covering the expected cool companion spectral features over the Y to K band domain
- Dual-polarization imaging (DPI) where the two quadrants of the detector image simultaneously two orthogonal linear polarization states.
- Classical imaging (CI) in a variety of narrow band to broad band filters from Y to K band
- Long slit spectroscopy (LSS) at low resolution (LRS) over Y-K band or at medium resolution (MRS) over Y-H band.

Is SPHERE the right instrument for your project?

This design can actually benefit to a wider range of astronomical observation purposes than exoplanet only. A few simple and important conditions under which you may be interested to use the SPHERE instrument:

- The residual non common path aberrations after phase diversity measurement and AO pre-compensation shall be lower than 0.8 (goal 0.4) nm per mode.
- AO system shall pre-compensate for 50 nm rms of non-common path defocus and 40 nm rms of the 55 first Zernike modes.

These values have been driven all the SAXO design.

The SAXO system is composed by 3 loops + one off line calibration

- Main AO loop (1.2 kHz): correct for atmospheric, telescope and common path defects. The main impact is the increase of detection signal to noise ratio through the reduction of the smooth PSF halo due to turbulence effects
- The DTT loop for fine centering on coronagraph mask (correction of differential tip-tilt between VIS and IR channel). It will ensure an optimal performance of the coronagraph device
- The PTT loop for pupil shift correction (telescope and instrument). It will ensure that the uncorrected instrumental aberrations effects (in the focal plane) will always be located at the same position and thus will be canceled out by a clever post-processing procedure
- NCPA pre-compensation which will lead to the reduction of persistent speckle [4]

3.2 Systeme performance with realistic conditions of turbulence

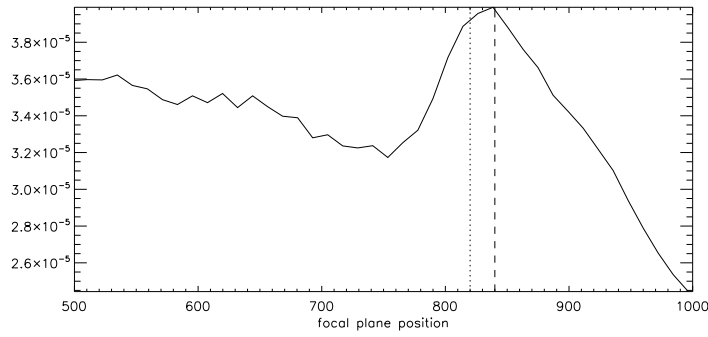
The SAXO nominal performance is define for the following conditions:

- $V_{mag} \sim 9$, i.e. 100 photo-e- per sub-aperture and per frame on the WFS (@1.2 kHz)
- Seeing = 0.85" and wind speed = 12.5 m/s

In these conditions, with a fully operational and optimized SAXO system (all loops closed, all optimization process "on" including Kalman Filtering on Tip Tilt) we have recorded classical PSFs and coronagraphic images on IRDIS (H2H3 mode).

Direct imaging will give us Strehl ratio and will allow us quantify AO loop residuals in terms of nm rms. The coronagraphic image will provide the final performance in terms of detectivity.

Before entering into a detailed analysis, it is important to quantify the impact of a TSIM defect which has NO impact on direct imaging and SR estimation but which introduce spurious effects on the coronagraphic image. It is described hereafter and a post processing modification is proposed to mitigate its impact. It has been called "the cloud effect".



Using a coronagraphic image we can estimate the cut off frequency using a circular average. Knowing the IRDIS image pixel scale we can derive a **corrected area of 1680 mas** (estimated using the bump maximum) which is fully coherent with the expected theoretical value of 1640 mas

Figure 2: Using a coronagraphic image we can estimate the cut off frequency using a circular average. Knowing the IRDIS image pixel scale we can derive a corrected area of 1680 mas (estimated using the bump maximum) which is fully coherent with the expected theoretical value of 1640 mas

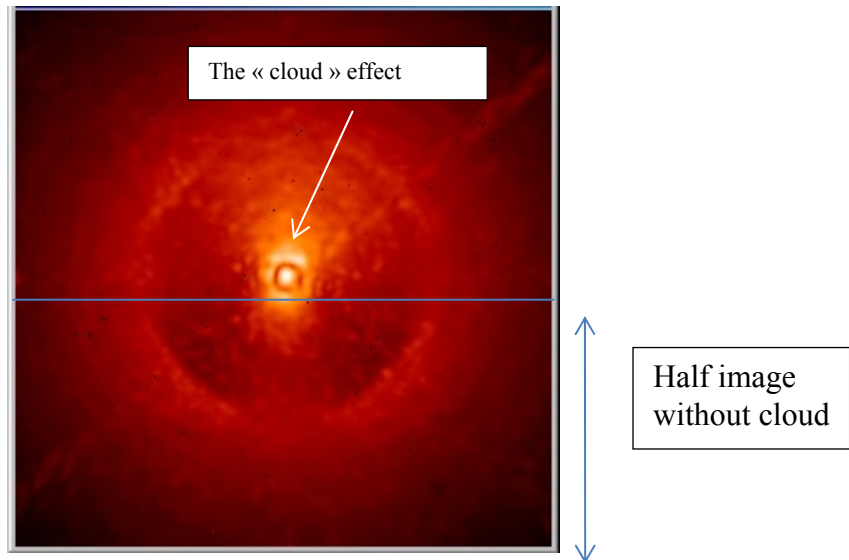


Figure 3 Coronagraphic image. Impact of the « cloud » on the up-side of the image

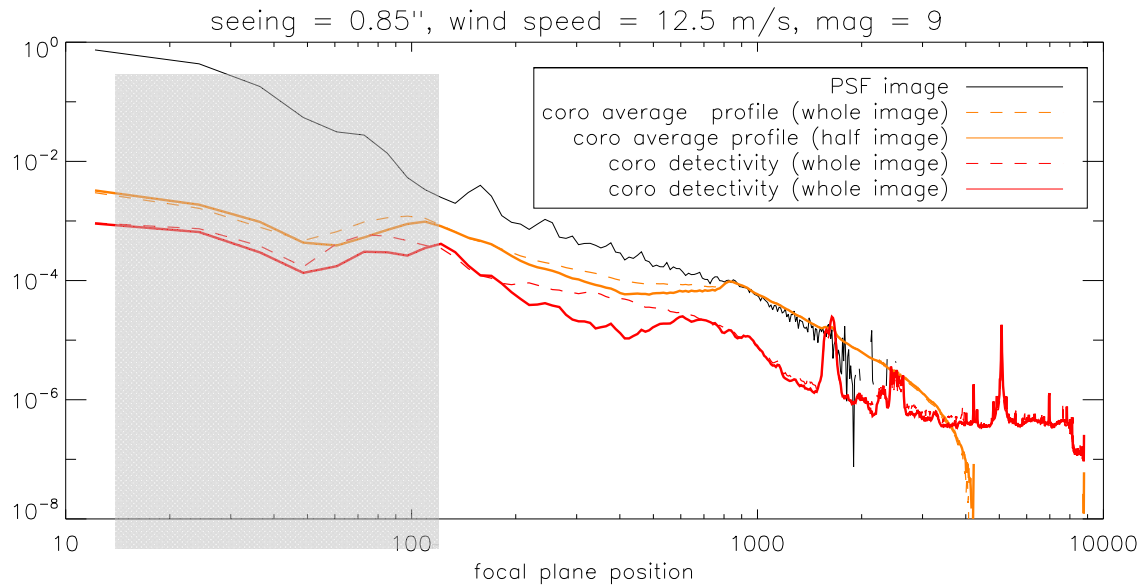


Figure 4 Comparison of circular mean [orange] and rms (detectivity) [red] of coronagraphic images.[dashed line] computation using the whole image, [solide line] computation using half image (without cloud).

IRDIS DBI mode has been extensively tested for the reference setup and the other setups, the conclusions for this mode are:

- It is fully functional for on-sky operation: hardware, templates, DRH, calibrations, performances have been validated;
- Tests have been performed with and without turbulence and show a level of performance compatible with technical specifications. Extrapolation of the lab performance to on-sky performance lead to the conclusion that IRDIS will be able to reach, the technical specifications of 10^{-5} @ 0.1" and 10^{-6} @ 0.5" under conservative assumption on ADI;
- A consistent scheme has been defined, implemented and validated for operation and calibrations.

The high priority reference setup for large survey for faint companion detection (H2H3, pupil-stabilized, one coronograph (ALC)) has been deeply tested. The performance of this mode is consistent with Technical Specifications if extrapolated using Angular Differential Imaging (ADI). Critical tests on telescope will be important to fully validate the technical specification with ADI (Time stability and ADC). While performance are non realistic in the laboratory tests, operation in ADI (INS Templates) and DRH have been fully validated.

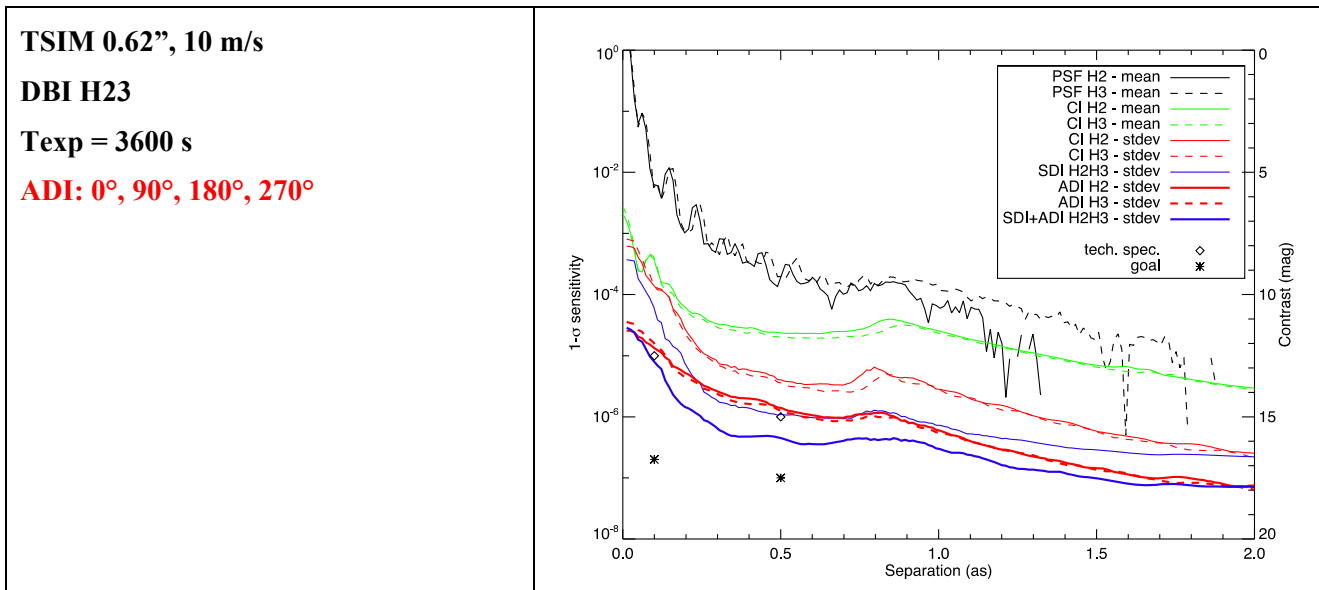


Figure 5: IRDIS performance in nominal turbulence conditions.

As can be seen from Figure 4, the current level of performance as obtained in laboratory does not reach the technical specifications of 10^{-5} @ $0.1''$ and 10^{-6} @ $0.5''$. However, the current state of the bench does not allow testing a close equivalent to angular differential imaging and/or reference star subtraction. Indeed, the VLT pupil is located in the TSIM located at the entrance of the instrument. Inducing a slow rotation of the derotator to simulation ADI-like data would result in a misalignment of the VLT pupil with the Lyot stop inside IRDIS, and stringly degrading the coronagraph performance. Three options have been investigated:

- 1- using discrete rotation of the derotator by multiples of 90° , which result in a maintained alignment between the VLT pupil and the Lyot stop;
- 2- using arbitrary rotation when observing with the internal point source, but in this case there is not VLT pupil in the optical path and there is no turbulence, which makes this case quite unrealistic ;
- 3- comparison to simulations to try extrapolating the lab detection limits to future on-sky detection limits.

Option 1 has been investigated in the test of Figure 4, in which 4 orientation of the derotator have been obtained. The data has been analysed using classical ADI, which means that the median of all the images has been subtracted to each of the images, and then derotation has been applied to bring all images to a common orientation. In case of combination with SDI, the SDI subtraction has been applied first before performing the classical ADI procedure. From this data it appears that the technical specifications can be reached in laboratory. Note however that in this test only the derotator is moving, contrary to the on-sky situation where the ADC will also be rotating.

4. FROM LAB TO SKY

The laboratory validation has been an important part of SPHERE validation. These validation included demonstration with a turbulent simulator, simulating the sky turbulence with various conditions.

The following table gathers some of the environment parameters that are different between laboratory and sky operation. The only parameters selected and shown in this table are those for which the sky operation is more constraining than the laboratory environment. This means that without precaution, the lab operation does not fully validate that the behavior on sky will meet the performance.

By instance, for temperature, the average value of temperature is around 20° in lab, 10° in paranal. The fainter temperature during sky operation is an asset, as the HODM shape at rest decreases with temperature. The system therefore is gaining robustness on sky, and demonstrating performance in lab is fully valid.

On the contrary, the temperature variation in lab is quite stable (around 1°), this will not be the case during sky operation, where temperature can vary from +5 to -5° during the night, hence involving some strong variation in HODM shape at rest. A dedicated action is under investigation in order to mitigate this effect, by the active constraint of a static optic (Torrice Mirror 3), with automatic compensation of thermal effects of HODM.

	Lab	Sky	Comment	Mitigation
Temperature	20°±1°	10°±5°	+Average temperature - Temperature evolution	Active TM3 for compensation of temperature-dependent aberrations
Turbulence	Stable r ₀ , wind	Unstable r ₀ and wind speed	- Not tested in lab	SAXO control law Optimised Modal Gain is able to adapt to turbulence level / wind speed.
Atmospheric dispersion	Non-dispersive atmosphere	Real sky	- Not tested in lab	

ADI + SDI performance	Via derotator angle, 0 90 180 270 °	Continuous 30°	Only derotator moving Large derotator angles	
Pupil alignment	Very good	Variation expected	-Strong impact on corono extinction	Pupil loop validated in lab
QuasiStatic Pattern	Not evolving with time	Will vary with time	-Impact on ADI performance	Daily calibration (Reference slopes, NCPA) Night calibration (corono centering and focus)
Operation	Fully automatised operation + pipeline	Fully automatised operation + pipeline		ESO standard environnement

Table 1: Environment parameters, differing between lab and sky. The impact of these parameter on laboratory validation is studied here.

5. CONCLUSION

The SPHERE instrument is now at the end of AIT phase and has demonstrated full performance in laboratory scheme. The demonstration of operational scheme is now ongoing. Acceptance visits are planned until the beginning of November 2013, preliminary acceptance is foreseen in November 2013. The first light of the instrument is foreseen in spring 2014.

REFERENCES

- [1] Beuzit, J.-L. , Mouillet, D. , Moutou, C. , Dohlen, K. , Puget, P. , Fusco, T. and Boccaletti, A., "A planet finder instrument for the VLT," Proc. of IAU Colloquium 200, Direct Imaging of Exoplanets: Science & Techniques, Cambridge University Press, pp. 317-323, (2005)
- [2] Bruce A. Macintosh ; Andre Anthony ; Jennifer Atwood ; Nicolas Barriga ; Brian Bauman et al " The Gemini Planet Imager: integration and status ", *Proc. SPIE* 8446, Ground-based and Airborne Instrumentation for Astronomy IV, 84461U (September 24, 2012); doi:10.1117/12.926721; <http://dx.doi.org/10.1117/12.926721>
- [3] Fusco, T. , Rousset, G. ,Sauvage, J.-F. ,Petit, C. , Beuzit, J.-L., Dohlen, K. , Mouillet, D., Charton, J. , Nicolle, M. , Kasper, M. , Baudoz, P. and Puget, P. , "High-order adaptive optics

requirements for direct detection of extrasolar planets: Application to the SPHERE instrument, " Opt. Express 14, 7515-7534 (2006)

[5] Sauvage, J.-F. , Fusco, T. , LeMignant, D. , Petit, C. , Sevin, A. , Dohlen, K. , Robert, C. , Mugnier, L. , "SPHERE non-common path aberrations measurement and pre-compensation with optimized phase diversity processes: experimental results," AO for ELT Proc., second edition, (2011)

[6] Kjetil Dohlen, Maud P. Langlois, Michel Saisse, "The infra red dual imaging and spectrograph for SPHERE: design and performance", in *Ground-based and Airborne Instrumentation for Astronomy II*, SPIE 7014-126 (2008)

[7] Riccardo U. Claudi, Massimo Turatto, Raffaele G. Gratton, Jacopo Antichi,; Enrico Cascone,; Vincenzo De Caprio,; Silvano Desidera, Dino Mesa, Salvatore Scuderi, "SPHERE IFS: the spectro differential imager of the VLT for exoplanets search", in *Ground-based and Airborne Instrumentation for Astronomy II*, SPIE 7014-119 (2008)

[8] Christian Thalmann, Hans M. Schmid, Anthony Boccaletti, David Mouillet, Kjetil Dohlen, Ronald Roelfsema, Marcel Carbillet, Daniel Gisler, Jean-Luc Beuzit, Markus Feldt, Raffaele Gratton, Franco Joos, Christoph U. Keller, Jan Kragt, Johan H. Pragt, Pascal Puget, Florence Rigal, Frans Snik, Rens Waters, Francois Wildi, "SPHERE ZIMPOL: Overview and performance simulation", in *Ground-based and Airborne Instrumentation for Astronomy II*, SPIE 7014-120 (2008)